

Modifications for the improvement of catalyst materials for hydrogen evolution

PERICA PAUNOVIĆ*, ORCE POPOVSKI, SVETOMIR HADŽI JORDANOV, ALEKSANDAR DIMITROV and DRAGAN SLAVKOV

*Faculty of Technology and Metallurgy, University “Sts Cyril and Methodius” Skopje and
*Military Academy “General Mihailo Apostolski” Skopje, R. Macedonia
(e-mail: shj@ereb1.mf.ukim.edu.mk)*

(Received 30 March, revised 13 June 2005)

Abstract: The structural and electrocatalytic characteristics of composite materials based on non-precious metals were studied. Precursors of metallic phase (Ni, Co or CoNi) and oxide phase (TiO₂) were grafted on a carbon substrate (Vulcan XC-72) by the sol–gel procedure and thermally treated at 250 °C. Ni and CoNi crystals of 10–20 nm were produced, in contrast the Co and TiO₂ were amorphous. The dissimilar electronic character of the components gives rise to a significant electrocatalytic activity for the hydrogen evolution reaction (HER), even in the basic series of prepared materials. Further improvement of the catalysts was achieved by modification of all three components. Hence, Mo was added into the metallic phase, TiO₂ was converted into the crystalline form and multiwall carbon nanotubes (MWCNTs) were used instead of carbon particles. The improvement, expressed in terms of the lowering the hydrogen evolution overpotential at 60 mA cm⁻², was the most pronounced in the Ni-based systems grafted on MWCNTs (120 mV lower HER overpotential) compared to 60 mV in case of Ni-based systems grafted on crystalline TiO₂ (TiO₂ prepared at 450 °C) and of Ni-based systems containing 25 at.% Mo. Nevertheless, even with the realized enhancement, of all the tested materials, the Co-based systems remained superior HER catalysts.

Keywords: composite electrocatalysts, hydrogen evolution, electronic interaction, real surface area.

INTRODUCTION

Due to its abundance and a number of other features, hydrogen is the most promising fuel in the field of alternative sources or energy.^{1–5} The use of hydrogen generated by water electrolysis, either in fuel cells or for heat generation, is characterized by high content of energy, absence of pollution (production of water as the by-product) and the possibility of creating a closed loop for its production and consumption. The main disadvantage of mass-scale production of hydrogen is the high

* Author for correspondence

specific energy consumption. The listed advantages make hydrogen generation by electrolysis a promising process for the future, regardless of the fact that presently this is not cost-competitive with respect to other technologies for hydrogen production, e.g., decomposition of natural gas.

In order to produce cheaper hydrogen by electrolysis, first of all the overpotential for the HER has to be lowered, *i.e.*, new electrode materials with improved electrocatalytic activity for the HER have to be developed.

Successful electrode materials for the HER have to satisfy a number of criteria. They have to be stable, *i.e.*, show no signs of corrosion or passivation in the long run, and to promote the HER. Economical reasons are in favor of cheaper materials, while environmental concern requests the use of non-polluting materials. Together these requests make the choice of an appropriate electrode material not an easy task, due to the conflict between the technical and economical issues.

Platinum was found to be an electrode material on the top of which hydrogen evolves with the minimum overpotential.⁶ Unfortunately, platinum, like other precious metals, is expensive. Alternative, non-precious metals, such as Ni, Co, *etc.*, are cheaper but suffer from corrosion, passivation and similar problems.

A number of investigations were concerned with the electrocatalytic activity of pure metals for the HER, in which attempts were made to correlate the basic parameters of electrode activity (exchange current density, i_0 or overpotential, η) with physical parameters, such as atomic number,^{7,8} M–H bond strength,^{9,10} work function,^{10,11} the so-called "d-character",^{12,13} electronegativity,¹⁴ melting and boiling point, heat of sublimation and vaporization,¹⁵ latent heat of both fusion and sublimation,¹⁶ *etc.* All these studies indicated that the intrinsic electrocatalytic activity is related to the electronic state of the metals. Nevertheless, an explicit dependence between these two parameters has not yet been given.

Attempts to improve the electrocatalytic activity of individual metals are concentrated on two basic approaches: (*i*) increasing the intrinsic catalytic activity by use of multicomponent catalysts and (*ii*) increasing the real surface area of the electrode, by use of porous electrodes or similar.

The need for active, stable and cheaper electrocatalysts motivated intensive research, which resulted in the development of multicomponent catalysts based on non-precious metals. The earliest successful attempts^{17–22} to combine non-precious metals from the right side of the transition series (certified as good individual catalysts) with metals from the left side (certified as poor individual catalysts) as catalysts for the HER did open a wide field of research in contemporary electrocatalysis. The components of the catalysts may be in the elemental or in valence state. The classification of different categories of these catalysts is given elsewhere.²³ Fundamental explanation of the synergetic effect achieved by combining transition metals and/or their compounds was given based on the Brewer valence-bond theory.^{24–26} In the light of this theory, strong bonding can be achieved

when the metal from the right side donates one or more electron pairs to form a chemical bond using the vacant d-orbitals of the metal from the left side. This results in the formation of stable intermetallic compound. The mutual sharing of d-orbitals provides an electronic configuration suitable for H⁺ adherence and transference. There is an analogy between the stability of the compound and the electrocatalytic activity, where extra-stable Laves phases of high symmetry show the highest catalytic activity for the HER.^{20,26}

An alternative approach for an explanation of the synergetic effect is based on the electronic structure of the alloys, in particular, the direction of electron transfer between atoms with dissimilar electronic character^{27–29} and its effect on the Fermi energy levels of the constituents. The electron density near a base metal atom (right side metal) is higher in the alloy than in the pure state, due to electron transfer from the surrounding atoms of the alloying metal (left side element). In this case, hydrogen evolution near the base metal atoms should be more favored in the alloy than in the pure base metal. Such a synergetic effect was proved in cases when the existence of a good correlation between the HER overpotential and the Fermi energy level²⁷ was confirmed.

The most practical approach for overcoming the kinetic and diffusional limitations is to increase the real surface area of the electrode. The real-to-geometric surface area ratio of Raney Ni-based electrodes³⁰ can reach 10000 to 12000. Gas-diffusion electrodes or membrane electrode assemblies (MEA) for PEM-type hydrogen generators are porous electrodes which use nanostructured particles of the electrocatalyst. In such a case, the left side metal (or its compound) plays a bifunctional role, both as a catalyst support and as a partner in the overall synergetic effect, due to the “strong metal-support interaction” (SMSI). SMSI has been termed by Tauster^{31,32} to account for the changes in the catalytic activity when metals of the VIII group are supported on TiO₂ in heterogeneous catalysis. Nanostructured catalysts require much stronger bonding supports, for both long-term stability and higher activity. In this respect titania has a unique role.^{31–33}

The aim of this work was to continue a previous study of the characterization of nonstructured composite electrocatalysts for hydrogen evolution. The basic catalyst systems were composed of TiO₂ as the oxide phase and Co, Ni or CoNi as the metal phase, deposited onto a carbon substrate by a precisely defined procedure. In this part, the effect of modification of the components of the catalyst aimed at improving their activity was the subject of interest.

EXPERIMENTAL

A simplified sol–gel procedure³⁴ was applied for the preparation of the composite catalysts. The catalysts consisted of three components – a carbon support with oxide and metallic phases. The procedure commences with the preparation of a mixed carbon–oxide phase support. Ti-isopropoxide (Aldrich, 97 %) was added to carbon Vulcan XC-72 (Cabot Corp. Boston Mass.) previously dispersed in anhydrous ethanol (p.a., Merck). To perform the conversion of Ti-isopropoxide to

Ti(OH)₄, 1 M HNO₃ was added in the ratio 1:10 based on the liquid phase. This mixture was evaporated at 60 °C under intensive stirring at 600–900 rpm until a fine non-scaled powder of catalyst support was obtained. Then the metallic phase was grafted onto the support. Individual or mixed Me-2,4-pentaedionate (Alfa Aesar, Johnson Matthey, GmbH) was dissolved in absolute ethanol. This solution was added to the dispersed support in absolute ethanol and this mixture was evaporated under the same conditions as above. The obtained powder was further thermally treated for 2 h at 250 °C under an atmosphere of H₂ and N₂, in order to calcinate Ti(OH)₄ to TiO₂ and to decompose any residual organometallics. The basic catalysts consisting of 10 % Me (Ni, Co or CoNi), 18 % TiO₂ and the rest of Vulcan XC-72 were prepared in this way.

Structural (XRD, SEM and BET) and electrochemical (cyclic voltammetry and steady-state galvanostatic method) characterization of the basic catalytic systems was carried out, the results of which were presented elsewhere.^{34–36}

In order to further improve the electrocatalytic characteristics, several modifications of components of the catalysts were made, *i.e.*:

i) Modification of the metallic phase. Mo was added to the metallic phase in an amount corresponding to the form MoNi₃ or MoCo₃. Molybdenyl acetylacetonate (MoO₂-acac, Aldrich) was used for this purpose.

ii) Modification of the oxide phase. Before grafting of the metallic phase, the catalysts support was heated at 480 °C in order to transform the amorphous TiO₂ into the crystalline anatase form of TiO₂.

iii) Modification of the carbon substrate. Instead of Vulcan XC-72, multi-wall carbon nanotubes (MWCNT) were used as the carbon substrate.

The compositions of the prepared catalysts are given in Table I.

TABLE I. The composition of the investigated electrocatalysts

Series	No.	Catalyst's components		
		Oxide phase (18 %)	Metallic phase (10 %)	Carbon substrate (72 %)
Basic	1	TiO ₂ (250 °C)	Ni	Vulcan XC-72
	2	TiO ₂ (250 °C)	Co	Vulcan XC-72
	3	TiO ₂ (250 °C)	CoNi	Vulcan XC-72
I Modif.	4	TiO ₂ (250 °C)	MoNi ₃	Vulcan XC-72
	5	TiO ₂ (250 °C)	MoCo ₃	Vulcan XC-72
II Modif.	6	TiO ₂ (480 °C)	Ni	Vulcan XC-72
	7	TiO ₂ (480 °C)	Co	Vulcan XC-72
	8	TiO ₂ (480 °C)	CoNi	Vulcan XC-72
III Modif.	9	TiO ₂ (250 °C)	Ni	Carbon nano tubes
	10	TiO ₂ (250 °C)	Co	Carbon nano tubes
	11	TiO ₂ (250 °C)	CoNi	Carbon nano tubes

The structural characteristics of the catalysts were determined by the X-ray diffraction method (XRD). The measurements were carried out on a XRD diffractometer Philips APD 15, with CuK_α radiation.

To compare the morphology of the catalysts deposited on both Vulcan XC-72 and carbon nanotubes, SEM observation was carried out using scanning electron microscope (JEOL, model JEM 200 CX).

Electrochemical characterization was performed by means of cyclic voltammetry and the steady-state galvanostatic method. Working electrodes (three-phase gas-diffusion electrodes) were prepared by hot pressing at 300 °C under a pressure of 300 kg cm⁻². They consisted of two layers: a back one of carbon black acetylene + PTFE and a front one of the catalysts + PTFE³⁷ (Fig. 1).

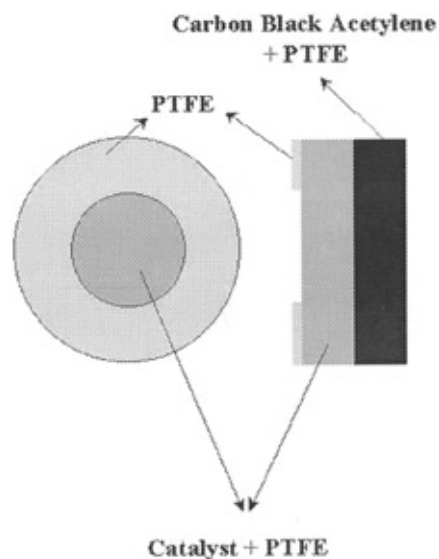


Fig. 1. Cross section of a three phase porous gas-diffusion electrode.

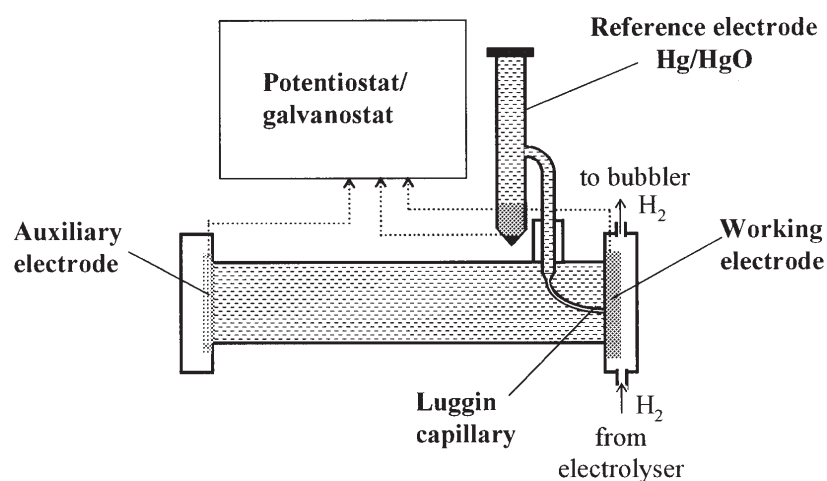


Fig. 2. Arrangement of the cell for the electrochemical measurements.

Electrochemical cell used for testing is shown in Fig. 2. A spiral shaped platinum wire was used as the counter electrode, while the reference one was Hg/HgO. The electrolyte was a solution of 3.5 M KOH (p.a., Merck) in ultrapurified water. During the electrochemical testing, a hydrogen steam was blown through the cathodic area. The measurements were performed using an AMEL electrochemical line (Function Generator AMEL 568, Potentiostat/Galvanostat 2053 and software package SOFTASSIST 2.0).

RESULTS AND DISCUSSION

The structural and electrochemical characteristics of the basic catalysts were presented elsewhere.^{34–36} The structural analysis showed that these catalysts contained a metal hyper phase of crystalline structure, of grain size 10–20 nm, except for

the Co-phase which was amorphous (grain size < 2 nm). In the mixed metallic system, a solid Co–Ni solution was also detected, which means that part of the Co substitutes Ni atoms in the Ni crystal lattice. A crystalline Ti-oxide phase was not detected by XRD. The overpotentials for the HER at a reference current density of 60 mA cm^{-2} were 275:290:485 mV, respectively for Co, CoNi and Ni based catalysts. Thus, the Co-containing catalyst was found to exhibit the highest catalytic activity.

Addition of Mo into the metallic phase

XRD Spectra of the catalysts with a modified metallic phase composition are shown in Fig. 3. The value of the cell parameter $a = 3.5419 \text{ \AA}$ for the MoNi_3 based catalyst is higher than the corresponding one of pure Ni ($a = 3.524 \text{ \AA}$). This implies the presence of a solid-state solution of Mo and Ni. The Ni peaks dominate the Mo ones, which indicates that the Mo atoms substitute Ni atoms in the Ni crystal lattice.

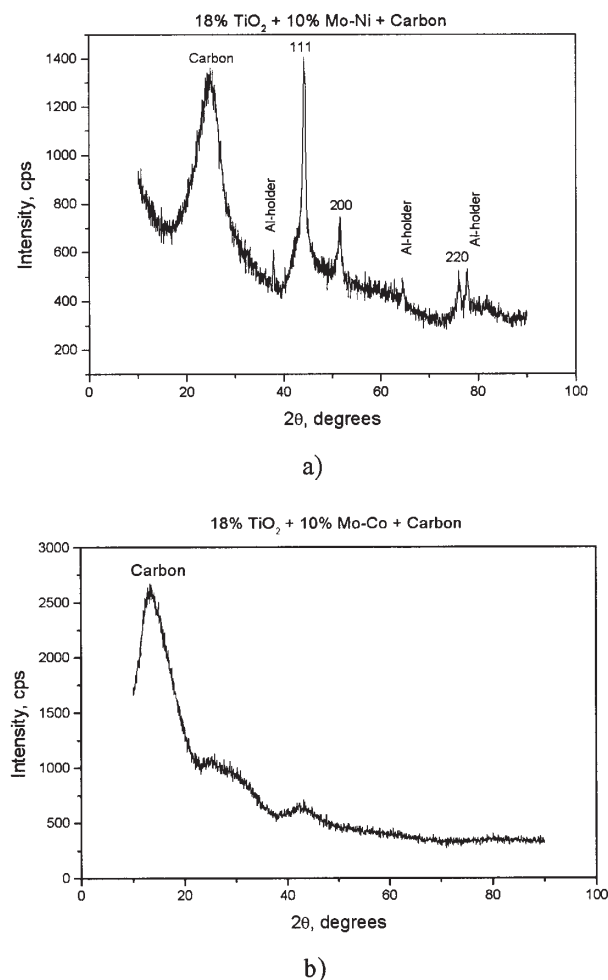


Fig. 3. XRD Spectra of catalysts containing 10 % Me + 18 % TiO_2 + Vulcan XC-72, (heated at $250 \text{ }^\circ\text{C}$): a) Me = Mo + Ni, Mo:Ni = 1:3 (at); b) Me = Mo + Co, Mo:Ni = 1:3 (at).

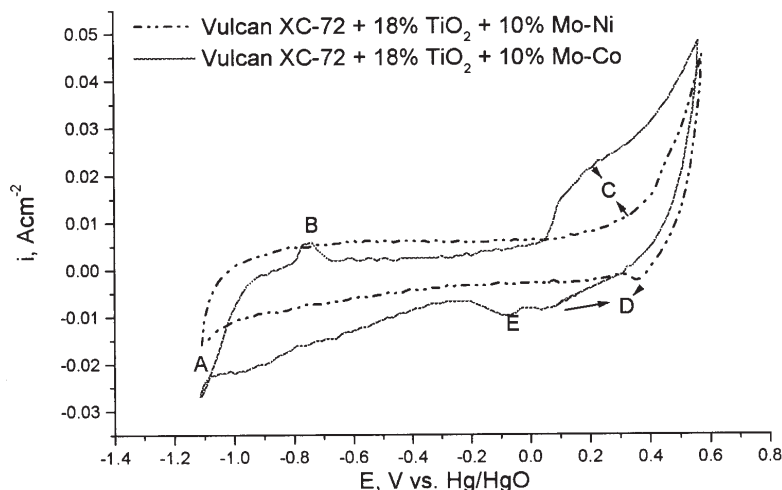


Fig. 4. Cyclic voltammograms of catalysts containing 10 % Me + 18 % TiO_2 + Vulcan XC-72, (heated at 250 °C). Me = Mo + Ni, Mo:Ni = 1:3 (at.) or Me = Mo + Co, Mo:Co = 1:3 (at.).

ce. According to EMPA analysis, the calculated atomic ratio of Ni/Mo \approx 3.8/1 implies the presence of MoNi_4 rather than MoNi_3 . However, only a solid-state solution of Ni and Mo with the cell parameter $a = 3.5419 \text{ \AA}$ was detected in the corresponding XRD spectrum. The size of the metallic crystallites was 10 nm. The crystalline state of the oxide phase was not detected, implying that the TiO_2 was amorphous.

The XRD pattern for MoCo_3 (Fig. 3b) contains low but very wide peaks, corresponding to particles of size less than 2 nm. This means that the MoCo_3 metallic phase was almost amorphous and phase identification is impossible. Crystalline TiO_2 was not detected, indicating that it was also amorphous.

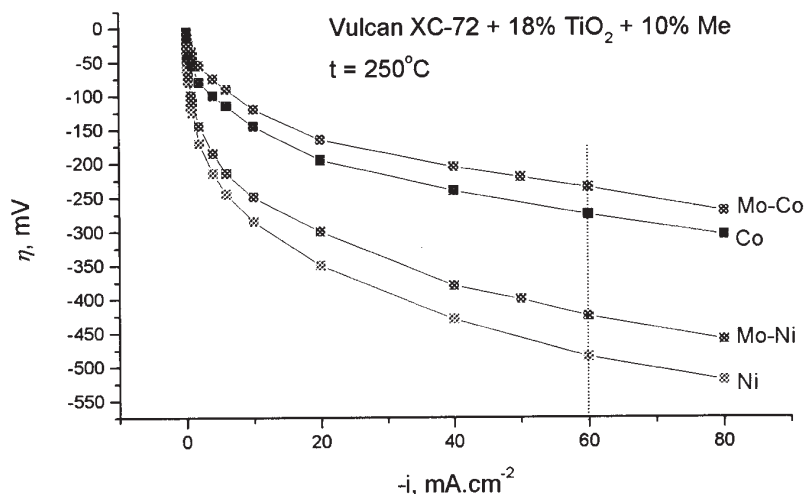


Fig. 5. Polarization curves, effect of the addition of 25 at. % Mo in the Ni or Co phase (10 % Me + 18 % TiO_2 + Vulcan XC-72).

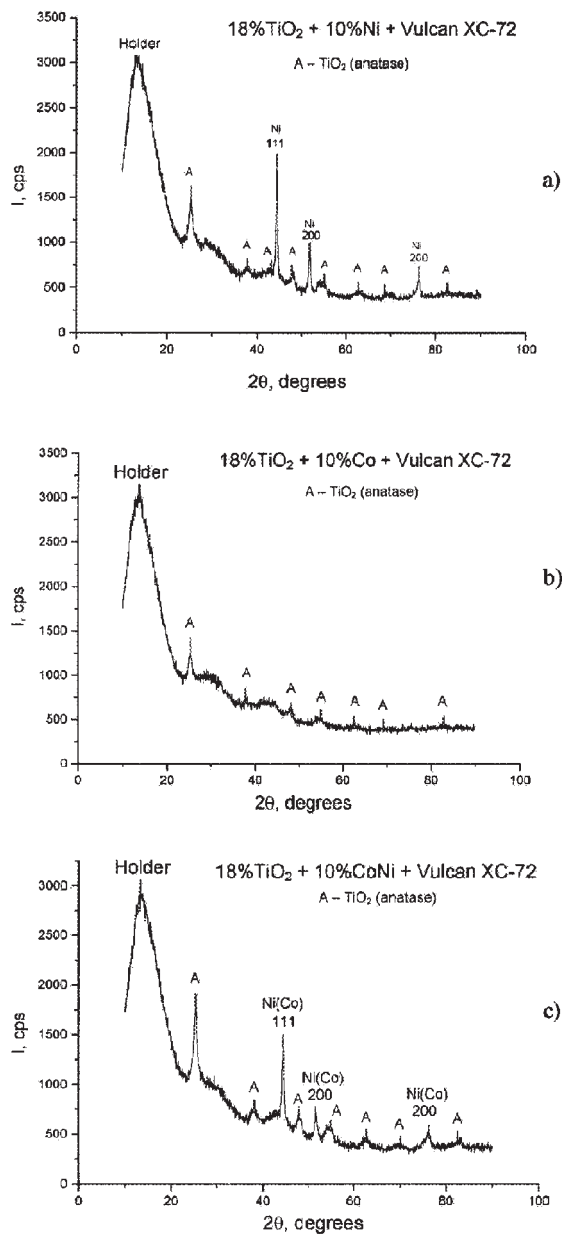


Fig. 6. XRD Spectra, effect of heating the TiO_2 at 480°C (10 % Me + 18 % TiO_2 + Vulcan XC-72): a) Me = Ni; b) Me = Co; c) Me = CoNi.

The cyclic voltammograms of this series are shown in Fig. 4. It is obvious that the MoCo_3 based catalyst is more active than the MoNi_3 one, according to the intensity of their peaks. Four different processes can be distinguished in these voltammograms. The peak B is attributed to the oxidation of $\text{Co}(0)$ to the $\text{Co}(\text{II})$ state and the further transformation of $\text{Co}(\text{II})$ to $\text{Co}(\text{III})$ is denoted by the peak C. Peaks D and E correspond to the reverse reduction of $\text{Co}(\text{III})$ to $\text{Co}(\text{II})$ and $\text{Co}(\text{II})$ to $\text{Co}(0)$, respectively.

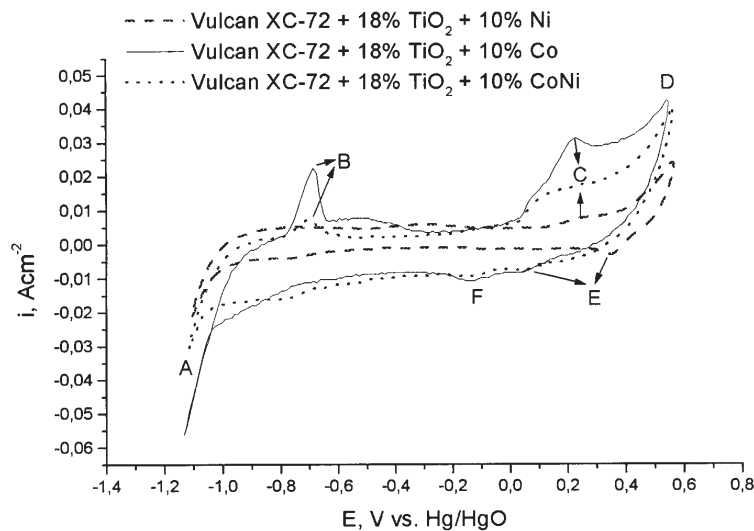


Fig. 7. Cyclic voltammograms of catalysts thermally treated at 480 °C (10 % Me + 18 % TiO₂ + Vulcan XC-72), Me = Ni, Co or CoNi.

The polarization characteristics of both the basic and modified catalysts are shown in Fig. 5. A considerable rise in the catalytic activity for the HER on addition of Mo into the metallic phase is evident. Taking the value of 60 mA cm⁻² as the reference current density, the overpotential of the MoCo₃ versus the Co based catalyst is lower by 40 mV, while the corresponding difference for the MoNi₃ versus the Ni catalyst is 60 mV.

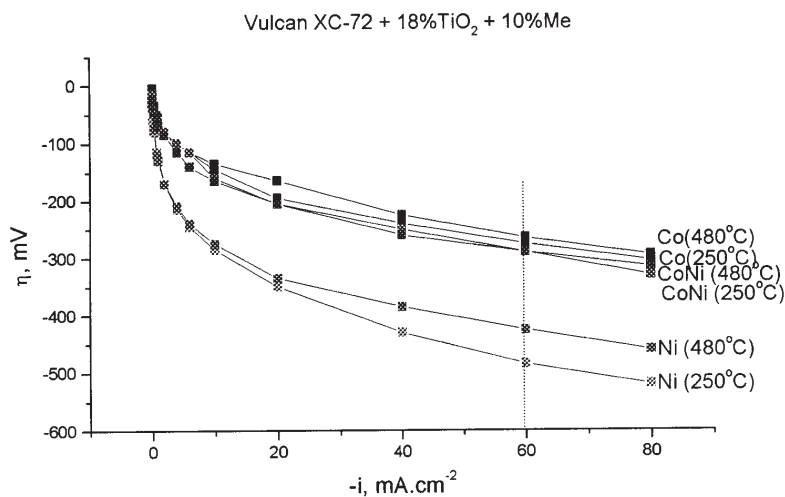


Fig. 8. Polarization curves, after heating the TiO₂ at 480 °C (10 % Me + 18 % TiO₂ + Vulcan XC-72), Me = Ni, Co or CoNi.

Transformation of amorphous titania into a crystalline form

Raising the temperature of thermal treatment up to 480 °C contributes to the transformation of the TiO₂ oxide phase from non-crystalline to a crystalline struc-

ture. This was detected by XRD-analysis. The XRD spectra for all the catalysts show peaks characteristic for anatase with a grain size of 7–8 nm (Fig. 6). The structural characteristics of the metallic phases were the same as those of the basic series, *i.e.*, Ni was crystalline, Co was amorphous, while in the Co–Ni system, a solid-state solution also existed. In the latter case, the dominant peaks correspond to Ni crystals, which means that some Co atoms were incorporated into the Ni crystalline cell. The Co “impurity” atoms substituted Ni host atoms in the local Ni crystalline environment and simultaneously, a structural phase transition of Co from amorphous to crystalline (as a solid-state solution) occurred. The rest amount of the Co remained amorphous.

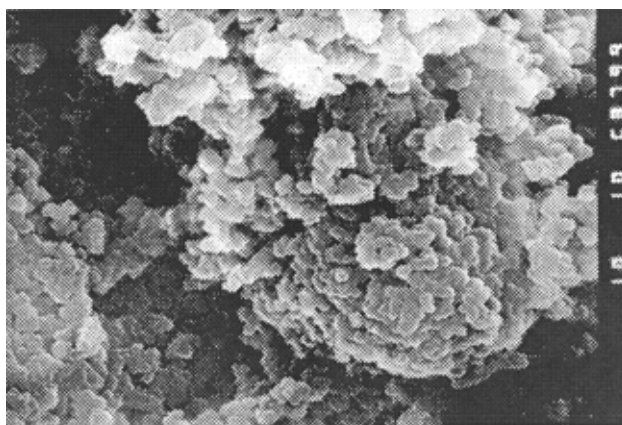
Cyclic voltammograms of the catalysts containing crystalline anatase are shown in Fig. 7. The voltammograms of the Co and CoNi based catalysts are very similar to that of the MoCo₃ one shown in Fig. 4. In the systems where Co was mixed with Ni or Mo, peaks characteristic for pure Co are dominant. The introduction of crystalline instead amorphous TiO₂ does not change significantly the voltammograms of the Ni based catalysts, as can be seen by comparing Fig. 7 and Fig. 4.

As can be seen from Fig. 8, the conversion of TiO₂ into its anatase structure increased activity of the catalyst. The overpotential difference of the catalysts thermally treated at 250 and 480 °C ($\eta_{250\text{ °C}} - \eta_{480\text{ °C}}$) for the HER is –15 mV for the Co based catalysts and even –60 mV for the Ni based ones, at the same reference current density as above. The polarization curve for the CoNi based catalyst almost overlaps with the curve of the corresponding catalyst of the basic series, meaning that no improvement of the catalytic activity was achieved.

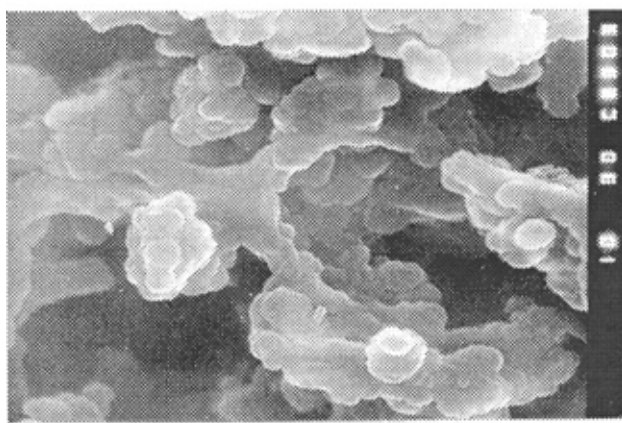
Carbon nanotubes as the carbon substrate

In order to increase both the active real surface area and the conduction characteristics of the catalysts, carbon nanotubes were used as the carbon substrate. As can be seen in Fig. 9a, the catalyst particles deposited on Vulcan were spherical in shape. The particles grouped into clusters of the *ca.* 100 nm, in which the adherence between the particles was good. Holes between the aggregates, contributing to a higher specific surface area, are only just evident. The catalysts deposited on CNT have an oriented structure (Fig. 9b). The spherical particles of the oxide and metallic phases are grafted onto the carbon tubes, which group into smaller clusters than was the case in Vulcan XC-72. This causes holes between the particles to appear. Due to their intrinsic geometrical shape (empty cylinders with a higher developed surface area as compared to the spherical particles of Vulcan XC-72 as well as with a higher inner porosity), CNT possess holes and the total surface area of the catalysts deposited on CNT is higher than the corresponding ones on Vulcan XC-72.

The values of the double layer capacity of the carbon nanotubes, as determined by cyclic voltammetry, were almost 2 times higher than those of Vulcan



a)



b)

Fig. 9. SEM Photographs, effect of the addition of carbon nanotubes (CNT), (10 % Ni + 18 % TiO₂ + C): a) C = Vulcan XC-72; b) C = CNT.

XC-72, *i.e.*, $C_{dl(CNT)} = 331 \text{ mF cm}^{-2}$ versus $C_{dl(Vulc.)} = 179 \text{ mF cm}^{-2}$. The double layer capacity was determined from a plot of current density (mA cm^{-2}) vs. change of scan rate (mV s^{-1}) in the potential region where only charging of double layer occurs. Without any doubt this is evidence that the CNT have considerably higher real surface area than Vulcan XC-72.

Cyclic voltammograms of the CNT containing catalysts are of the same shape as those of the reference one, but with more pronounced peaks and higher current densities.

According to the relative position of the polarization curves in Fig. 10, it is obvious that the most effective improvement of the catalytic activity was achieved by using carbon nanotubes as the carbon substrate. For the Co system, the overpotential of hydrogen evolution at 60 mA cm^{-2} was lowered by -25 mV , for the CoNi system by -20 mV and for the Ni system as much as -120 mV . This enhancement was caused mainly by the increase of the real surface area and the better conduction characteristics of the carbon nanotubes.

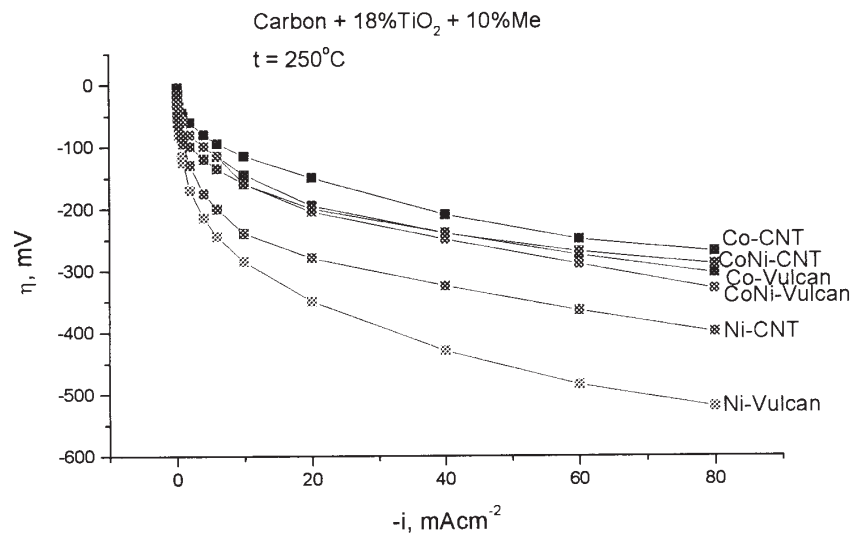


Fig. 10. Polarization curves, effect of the addition of carbon nanotubes (CNT), (10 % Ni + 18 % TiO₂ + C), C = Vulcan XC-72 or CNT, Me = Ni, Co or CoNi.

General discussion

In this study, the basic catalysts were modified in order to improve their electrocatalytic characteristics for the HER. An increase of both the electronic interaction between the components of the catalysts with dissimilar electronic character and the active surface area was achieved. Addition of Mo into the metallic phase and transformation of TiO₂ into its crystalline anatase form resulted in an increase of the interaction between the compounds of the catalyst *i.e.*, an increase of the electronic density of the composites. In the former case, besides the interaction of the metal phase (Co, Ni or CoNi) with TiO₂, there is an additional d-electronic interaction with Mo. Transformation of TiO₂ into its crystalline state intensifies its electronic interaction with the metallic phase. Introduction of CNT results in a significant increase of the real surface area and of the electronic conductivity. In addition, the structural characteristics of the metallic phases play a significant role in the improvement of the catalytic activity. For a better understanding of the effects of the applied modifications, each metallic system is discussed separately.

The overpotentials for the HER on the modified catalytic systems are compared in Table II with the ones of the corresponding basic series. The resulting decrease in the overpotential is also given in Table II.

Catalysts based on a Co metallic phase were found to be the most active ones in both basic and modified series. On the other hand, these systems exhibited a less developed BET surface area. These facts raise the question of how it is possible that the system with the lowest surface area exhibits the maximal catalytic activity.

Firstly, the BET determinations were made on completed catalytic systems and the obtained values represent the area of all the components of the system, *i.e.*, carbon sub-

strate, TiO₂ and metal phase. The catalytic activity of such a system depends mainly on the activity of the metallic phase, thus on the intrinsic activity and surface area of the metal phase. Hence, the Co systems may be superior to the CoNi and Ni systems due to both a higher catalytic activity and/or a more developed surface of the metallic phase only. The former possibility does not hold because the intrinsic activity of Co and Ni metallic phases are practically identical. The measured values of the total surface area are 70:90:108 m² g⁻¹ for the Co:CoNi:Ni based catalysts, respectively.²³ The approximately 50 % higher surface area of Ni containing system could easily be compensated for by more developed surface area of the metallic phase particles (2 nm of Co particles vs. 20 nm of Ni particles). Nevertheless, the addition of Co minimizes the surface area of the whole aggregate, despite the fact that Co itself is amorphous, *i.e.*, has the most developed surface. For the Co-containing catalysts, the modifications applied in this study do not produce any marked rise in the activity, probably due to the fact that the activity was already maximized, mainly due to the amorphous state of the Co phase. Addition of Mo in case of the Co based catalyst resulted in drop of the overpotential by -40 mV, probably due to the double interaction between Co and TiO₂, as well as Co and Mo, thus resulting in a higher catalytic activity. Modification of the amorphous TiO₂ into crystalline anatase, as well as the substitution of Vulcan XC-72 with CNT had no significant effect with the Co-system. The measured drop of the HER overpotentials were -15 mV and -25 mV, respectively.

TABLE II. Overpotential for the hydrogen evolution reaction on the investigated catalysts at 60 mA cm⁻² and the overpotential difference with respect to the corresponding catalysts of the basic series

Series	No.	Metallic phase	η / mV	$\Delta\eta$ / mV
Basic	1	Co	-275	-
	2	CoNi	-290	-
	3	Ni	-485	-
I Modif.	4	MoCo ₃	-235	40
	5	MoNi ₃	-425	60
II Modif.	6	Co	-260	15
	7	CoNi	-290	0
	8	Ni	-425	60
III Modif.	9	Co	-250	25
	10	CoNi	-270	20
	11	Ni	-365	120

The Ni-containing catalysts were shown to be the least active of all the basic systems. For this reason, the modifications caused by the addition of Mo and crystalline TiO₂, as well as of CNT are more remarkable in the case of the Ni-catalysts. The corresponding overpotential drops were -60 mV, -60 mV and -120 mV, respectively. Despite the fact that the complex system (*i.e.*, carbon + TiO₂ + Me) were found to exhibit the highest developed surface area in the case of Ni, their ac-

tivities as catalysts for the HER were inferior to those of the Co and CoNi systems. The measured size of the Ni grains was 10–20 nm, which indicates that the electrocatalysis was enabled by the underdeveloped surface area.

The CoNi-containing catalysts have a specific feature, very similar to the systems containing Co only. The XRD analysis as well as the results presented elsewhere³⁹ indicate that Co in this case exists in two different phases. A minor part of it forms a Ni–Co solid state solution while the rest continues to exist as pure (amorphous) Co, thus maintaining the superior activity typical for the pure Co-system.

Three dimensional gas-diffusion electrodes could possibly acquire lower activity at higher current densities (as compared to, *e.g.*, Raney-Ni or Raney-Ni activated electrodes) due to the nature of their structure. If the evolved hydrogen could not escape out of the subcritically sized pores, then the operating surface area (of such 3D electrodes) is lower than the real one. A similar phenomenon was found and discussed by Wendt and coworkers.^{40,41} According to them, even as much as 90 % of the surface area available for hydrogen evolution could be blocked and become inactive. Probably a similar situation exists with the present electrodes. Engineering aspects of the electrodes are going to be the subject of study in some further investigations, and are not included in this paper.

In case of two-phase membrane electrodes, as PEM cells are, such limitations are not encountered, due to the absence of a liquid phase, capture of hydrogen is for less possible because bubbles do not exist.

CONCLUSION

Despite the fact that the invention and the development of non-precious metals based electrocatalysts for the HER was founded on an extensive fundamental research (aimed at understanding the correlation between the discrete structure of the chemical elements and a number of their properties, especially the ones responsible for hydrogen adsorption/desorption) there is still sufficient space for empirical research. In this paper three modifications of the preparation procedure of Co, CoNi and Ni based catalysts for the HER were applied and their effects on both structural and electrocatalytic characteristics were studied.

The starting catalytic materials were prepared under a more or less standard procedure described elsewhere.³⁴ The modification consisted of (*i*) introducing Mo into the Co and Ni metal as a metallic component, (*ii*) transformation of amorphous TiO₂ into a crystalline form and (*iii*) substitution of carbon powder (Vulcan XC-72) with carbon nanotubes. The choice of these modifications is not at all accidental, but was based on previous experience and some results achieved by such and/or similar options. For this reason all three modifications appeared to be successful.

Hence, the addition of Mo in amounts corresponding to the atomic ratios in MoCo₃ and MoNi₃ lowers the overpotential by 40 mV for the Co system and 60 mV for the Ni one.

The effect of converting TiO_2 from the amorphous into a crystalline state results in a decrease in the overpotential by 15 mV for the Co based catalyst and 60 mV for the Ni one.

The effect of using CNT instead of Vulcan XC-72, was the most successful. The overpotential decreases, by 25 mV in the case of the Co system, 20 mV for the CoNi and as much as 120 mV for the Ni one.

Finally, it can be concluded that the investigated catalytic systems are rather complex and it can practically never be stated that the best of their performance was achieved. Modifications like these (or other) will probably be further visioned and applied, just contributing to a further, fast or slow, but in any case a continuous increase of the catalytic activity for the HER.

Acknowledgements: This paper was supported by and carried out within the EU Project "PROMETHEAS" PL ICA2-2001-10037. Cooperation with the "Institute of Electrochemistry and Energy Systems", Bulgarian Academy of Science, Sofia is gratefully acknowledged. The continuous interest and help of Prof. M. Jakšić in the progress of this research is also gratefully appreciated.

ИЗВОД

ПОСТУПАК ЗА УСАВРШАВАЊЕ КАТАЛИТИЧКИХ МАТЕРИЈАЛА ЗА ИЗДВАЈАЊЕ ВОДОНИКА

ПЕРИЦА ПАУНОВИЋ, ОРЦЕ ПОПОВСКИ, СВЕТОМИР ХАЦИ ЈОРДАНОВ, АЛЕКСАНДАР ДИМИТРОВ и ДРАГАН СЛАВКОВ

Технолошко-металуришки факултет, Универзитет "Св. Кирил и Методије", Руѓер Бошковић 16, 1000 Скопје и Војна академија "Генерал Михаило Апостолски", 1000 Скопје, Р. Македонија

Испитиване су структурне и електрокаталитичке карактеристике материјала на бази неплеменитих метала, који су намењени за израду електрода за издвајање водоника. Израда материјала је вршена поступком где се метална фаза (Ni, Co или CoNi) заједно са оксидном фазом (TiO_2) равномерно распоређује поврх проводљиве подлоге од угљеничног материјала Vulcan XC-72. Различити електронски карактер коришћених метала (металних једињења) омогућава знатну електрокаталитичку активност, а у неким случајима чак и појаву синергизма. Поступак припреме материјала је такав да су металне фазе Ni и CoNi у кристалном облику (величине зрна 10–20 nm), док је метални Co аморфан са величином зрна мањом од 2 nm. Аморфне структуре су и честице TiO_2 које су добивене загревањем прекурсора на 250 °C. У овом раду је испитиван ефекат модификације састава електродног материјала на његове структурне и електрохемијске особине. Тако, утврђено је да додаток Mo у металну фазу побољшава каталитичку активност. Коришћењем једињења MoCo_3 уместо чистог Co, као и MoNi_3 уместо чистог Ni, на –235, пренапетост издвајања водоника са густином струје од 60 mA cm⁻² снижава се са –275 mV (RHE), односно са –485 на –425 mV, респективно. Претварање аморфног TiO_2 у кристални облик анатаза што се постиже загревањем прекурсора на 480 °C), одговарајући пренапетости кад исте референтне густине струје се смањују за 15 mV код електрода са кобалтом и за 60 mV код електроде базиране на никелу.

Употреба угљеничних наноцевчица (CNT) уместо прашка Vulcan XC-72 је најделотворнија модификација. Овакве електроде показују пренапетост нижу за 25 mV код Co-система и за читавих 120 mV код Ni-система.

(Примљено 30. марта, ревидирано 13. јуна 2005)

REFERENCES

1. J. O'M Bockris, in *Electrochemistry in Cleaner Environment*, J. O'M Bockris, Ed., Chapter 1, Plenum Press, New York, 1972
2. J. O'M Bockris, D. Dražić, *Electrochemical Science*, Taylor & Francis, London, 1972
3. A. R. Despić, in *Electrochemistry: The Past Thirty and the Next Thirty Years*, H. Bloom and F. Gootman, Eds., Plenum Press, New York, 1977, p. 9
4. C. Mitsugi, A. Harumi, F. Kenzo, *Int. J. Hydrogen Energy* **23** (1998) 159
5. P. Kruger, *Int. J. Hydrogen Energy* **25** (2000) 395
6. H. Kita, in *Electrochemistry: The Past Thirty and the Next Thirty Years*, H. Bloom and F. Gootman, Eds., Plenum Press, New York, 1977, p. 117
7. H. Kita, *J. Electrochem. Soc.* **113** (1966) 1095
8. M. H. Miles, *J. Electroanal. Chem.* **60** (1975) 89
9. L. I. Krishtalik, in *Advanced Electrochemistry and Electrochemical Engineering*, H. Gerisher and C. W. Tobias, Eds., Vol. 7, Wiley, New York, 1970, p. 283
10. S. Trasatti, *J. Electroanal. Chem.* **39** (1972) 163
11. S. Trasatti, in *Advances in Electrochemistry and Electrochemical Engineering*, H. Gerisher and C. W. Tobias, Eds., Vol. 10, Interscience, New York, 1977, p. 213
12. B. E. Conway, J. O'M Bockris, *Nature* **178** (1956) 488
13. B. E. Conway, J. O'M Bockris, *J. Chem. Phys.* **26** (1957) 532
14. S. Trasatti, *J. Chem. Soc. Faraday Trans* **68** (1972) 229
15. H. Kita, *J. Res. Inst. Catal. Hokkaido Univ.* **21** (1973) 200
16. A. T. Khun, C. J. Mortimer, G. C. Bond, J. Linley, *J. Electroanal. Chem.* **34** (1972) 1
17. V. Komnenić, *M. Sc. Thesis*, Centre for Multidisciplinary Studies, University of Belgrade, Belgrade, 1974
18. M. M. Jakšić, V. Komnenić, R. Atanasoski, R. Adžić, *Elektrokhimiya* **13** (1977) 1355
19. K. Mund, G. Richter, F. von Sturm, *J. Electrochem. Soc.* **124** (1977) 1
20. T. Kitamura, C. Iwakura, H. Tamura, *Electrochim. Acta* **27** (1982) 1723
21. K. Machida, M. Enyo, I. Toyoshima, K. Miyahara, K. Kai, K. Suzuki, *Bull. Chem. Soc. Jpn.* **56** (1983) 3393
22. K. Machida, M. Enyo, K. Oguro, M. Nakane, *Bull. Chem. Soc. Jpn.* **57** (1984) 2809
23. S. Hadži Jordanov, P. Paunović, O. Popovski, A. Dimitrov, D. Slavkov, *Bull. Chem. Technol. Macedonia* **23** (2004) 101
24. L. Brewer, in *Electronic Structure and Alloy Chemistry of Transition Elements*, P. A. Beck, Ed., Interscience, New York, 1965, p. 221
25. M. M. Jakšić, *Electrochim. Acta* **29** (1984) 1539
26. M. M. Jakšić, *Int. J. Hydrogen Energy* **12** (1987) 727
27. H. Ezaki, M. Morinaga, S. Watanabe, *Electrochim. Acta* **38** (1993) 557
28. H. Ezaki, M. Morinaga, S. Watanabe, J. Saito, *Electrochim. Acta* **39** (1994) 1769
29. H. Shibutani, T. Higashijima, H. Ezaki, M. Morinaga, K. Kikuchi, *Electrochim. Acta* **43** (1998) 3235
30. S. Tanaka, N. Horise, T. Tanaki, Y. Ogata, *J. Electrochem. Soc.* **147** (2000) 2242
31. S. J. Tauster, S. C. Fung, *J. Catal.* **55** (1978) 29
32. S. J. Tauster, S. C. Fung, R. L. Garten, *J. Am. Chem. Soc.* **100** (1978) 170
33. S. G. Neophytides, S. Zaferiatos, G. D. Papakonstantinou, J. M. Jakšić, F. E. Paloukis, M. M. Jakšić, *Int. J. Hydrogen Energy* **30** (2005) 131
34. P. Paunović, O. Popovski, V. Nikolova, P. Iliev, M. Tasev, E. Lefterova, *XVIIIth Congress of Chemists and Technologists of Macedonia*, Ohrid (2004) ECH-1
35. P. Paunović, O. Popovski, A. Dimitrov, D. Slavkov, M. Tasev, S. Hadži Jordanov, *XVIIIth Congress of Chemists and Technologists of Macedonia*, Ohrid (2004) ECH-2
36. P. Paunović, O. Popovski, A. Dimitrov, D. Slavkov, M. Tasev, S. Hadži Jordanov, *XVIIIth Congress of Chemists and Technologists of Macedonia*, Ohrid (2004) ECH-3

37. BG patent Appl. No 38581P
38. A. D. S. Tantram, A. C. C. Tseung, *Nature* **222** (1969) 556
39. Y. L. Soo, G. Kioseoglou, S. Kim, Y. Kao, P. Sujatha Devi, J. Parise, R. J. Gambino, P. I. Gouma, *Appl. Phys. Lett.* **81** (2002) 655
40. S. Raush, H. Wendt, *J. Electrochem. Soc.* **143** (1996) 2852
41. Th. Borucinski, S. Rausch, H. Wendt, *J. Appl. Electrochem.* **22** (1992) 1031.